

GLOBAL EMISSION MONITOR FOR 2023

Abstract

This study creates a global emission monitor for 2023 composed of an emission inventory as well as further analyses. Automatic Dependent Surveillance–Broadcast (ADS-B) data is leveraged to derive a comprehensive analysis of flight trajectories, encompassing all aviation operational sectors. Schedule and flight trajectory data, combined with aircraft performance characteristics and meteorological information, are used to construct a global aviation emission inventory for the year 2023. Due to the lack of detailed global cargo flight schedules, a dedicated cargo flight plan is derived, to better understand the cargo sector. Furthermore, ADS-B data is used to assess the aviation system responses to geopolitical conflicts and natural hazards.

Keywords: aviation emission inventory 2023, ADS-B data, air transport, air cargo traffic, impact assessment

1. Introduction

Global aviation's impact to anthropogenic climate change is about 3.5 % [1] while the number of passengers is expected to increase by 3.1 % per annum until 2070 [2]. At the same time, decarbonisation in aviation is more challenging than in other modes of transport due to technological, operational, and infrastructural constraints and limitations. Since operational inefficiencies contribute significantly to aviation emissions, and the climate effects of these emissions strongly depend on their location and timing, accurately capturing real-world flight behaviour has become increasingly important. The introduction of Automatic Dependent Surveillance–Broadcast (ADS-B) has enabled the systematic observation of actual aircraft trajectories, allowing real-world operational behaviour to be represented with high spatial and temporal resolution. Beyond improving the accuracy of scheduled traffic representation, ADS-B data also facilitate the inclusion of flight operations and aviation sectors for which no comprehensive global databases exist, such as general aviation, cargo traffic, and military and governmental flights, all of which may contribute a substantial share of global aviation emissions. Current studies, computing global emission inventories with bottom-up approaches, consider the time horizon until 2021 and cover global traffic either based on ADS-B data [3, 4, 5], scheduled flight plan data in combination with ADS-B data for more realism [6] or lastly only scheduled flight plan data without any detailed flight trajectories [7, 2]. Bottom-up approaches simulate each flight individually while top-down approaches use estimates for global jet fuel consumption and deriving conclusions regarding individual flights is not possible. The emissions' location is furthermore relevant for the non-CO_2 climate effect of aviation emissions. A major research gap is the limited consideration of cargo air traffic in existing forecasts due to a limited availability of complete cargo flight data. Furthermore, multiple geopolitical conflicts lead to certain airspace closures which lead to increased lateral inefficiencies as well as possible competitive disadvantages [3, 8] Therefore, this study quantifies the fuel consumption and emissions associated with each individually identifiable flight by incorporating meteorological reanalysis data and historical flight trajectories derived from an ADS-B dataset for the year 2023. The resulting dataset is subsequently utilized to:

1. Develop a global aviation emission inventory based on actual flight trajectories,
2. Derive a global cargo flight plan to improve the quantification of the environmental impact of cargo aviation and to support future forecasting applications,

https://doi.org/10.71945/icas2026_0666

3. Analyze lateral routing inefficiencies between world regions under constrained and unconstrained airspace.

Firstly, the data used for this study and methods are described in section 2.. In section 3. the results are presented and discussed before completing with the conclusion and outlook in section 4..

2. Data and methods

The data sources and methodologies employed in the development of the global emission inventory are described in detail in the following chapter. First, the ADS-B data source is introduced (2.1), followed by a description of the meteorological data utilized (2.2). Finally, the chapter concludes with the aircraft performance- emissions and trajectory modelling approach (2.3).

2.1 Air traffic schedule and trajectory data

This study utilizes a global ADS-B dataset with a temporal resolution of 30 s for the year 2023, provided by Spire Global [9], to reconstruct detailed flight trajectories and derive the associated flight plans. The dataset further includes operational and aircraft-specific metadata, such as flight numbers, scheduled origin and destination airports, and scheduled departure and arrival times. As part of the preprocessing workflow, individual ADS-B data points are aggregated into continuous flight trajectories using a multi-criteria assignment procedure and subsequently associated with unique flight identification numbers. The resulting origin-destination (OD) airport assignments are validated and corrected to account for diversions, interrupted trajectories, and potential misclassifications. For flights with incomplete trajectory data due to ADS-B coverage limitations, departure- or destination airports are estimated based on geographical proximity and trajectory consistency. The positional variables latitude, longitude, and altitude are subsequently subjected to outlier detection and smoothing procedures. Aircraft are categorized according to their engine type, turbofan, turboprop, and piston-engine using either the International Air Transport Association (IATA) aircraft code or the full aircraft type designation. Cargo aircraft are identified primarily through the aircraft type designation (e.g. Boeing 777-FZN), as classification approaches relying solely on an aircraft's IATA code in combination with the airline may not provide sufficient robustness. Data obtained by Sabre Market Intelligence [10] as well as Cirium [11] is used to cross validate the obtained meta data to compare the detected air traffic with the scheduled passenger traffic.

2.2 Meteorological data

To calculate the air distance, wind information from the ERA5 reanalysis dataset provided by the European Centre for Medium-Range Weather Forecasts (ECMWF) is used [12]. To reduce computational complexity and storage requirements, only data from 00 UTC and 12 UTC for each day of the year 2023 is used. The reanalysis data has a horizontal resolution of $0.25^\circ \times 0.25^\circ$. Vertically, the dataset is resolved in 100 hPa intervals from 1 000 hPa to 500 hPa, while all available pressure levels are used between 450 hPa and 125 hPa. For each flight, the wind field closest in time to the temporal midpoint of the flight is selected. Wind values at each waypoint are then obtained using linear interpolation within the wind field. Although this simplification has a major impact on lower flight levels, most fuel is burned in cruise flight in proximity to the tropopause. Tropopause-level winds are governed by synoptic-scale atmospheric dynamics. Hence, their structure typically evolves over periods of days rather than hours, changes within a 12-hour window are generally limited.

2.3 Aircraft performance- emissions and trajectory modeling

Emission quantities and locations are calculated with the DLR Global Air Traffic Emission Distribution Laboratory (GRIDLAB) [13, 6] which uses multiple different input datasets. Detailed 4D flight trajectories are modelled with the Trajectory Calculation Module (TCM) [13, 14]. The TCM uses the total-energy-model and aircraft specific flight performance data provided by BADA4 (version 4.2) from EUROCONTROL [15], German Aerospace Center (DLR) internal data [16] or the Poll-Schumann-Model [17]. To enable efficient computation of large-scale emission inventories, standardized reduced emission profiles (RedEmP) are employed to estimate aircraft fuel flow, flight physics parameters such as true airspeed, and emissions along flight trajectories. RedEmPs are precomputed datasets

of key flight performance parameters defined for standardized trajectories for discrete flight lengths, in 100 NM steps, various cruise flight levels and seat load factors [18, 19]. Engine degradation effects on the fuel consumption are not considered which increase fuel consumption by about 2.25 % over an engines life time [20]. Each RedEmP specifies the flight performance parameters at the boundary points of the individual flight phases.

For application to real flights, the profiles are scaled to match the air distance of each flight while accounting for the actual trajectory and prevailing wind conditions. During the gridding process, emissions are distributed among the grid cells according to the travelled air distance within each cell. Additionally, BADA3 (version 3.11) is used with a forward integration to compute additional aircraft types that are not included in the RedEmP database. For the estimation of CO_2 and H_2O emissions, constant emission factors of 3.159 kg CO_2 and 1.237 kg H_2O per kg fuel are applied [21], while life-cycle impacts associated with sustainable aviation fuel usage are not considered. Regional averages of fuel sulphur content data for the year 2010 are taken from the Coordinating Research Council [22] to derive SO_2 emissions. Non-linear emissions of CO and unburned hydrocarbons (HC) are calculated using the Boeing Fuel Flow Method 2 [23] in combination with ICAO's Engine Emissions Databank (EEDB) version 31 [24]. Nitrogen oxide emissions (NO_x) are derived as NO_2 mass equivalents using the DLR methodology [25, 24]. The Aircraft nvPM Mission Emissions Estimation Methodology, Version 2 (MEEM2) in combination with the EEDB is used to calculate the non-volatile particle matter (nvPM) emissions [24, 26]. In case of missing nvPM emission measurements, the SCOPE11 method is used to estimate the LTO emission indices based on the smoke number for each thrust setting [27]. In case the smoke number is not present, a constant emission index of $10^{15} \frac{\#}{\mathrm{kg_{fuel}}}$ is considered. The overall workflow is explained in detail in Righi et al. (2026) [6]. First, for each scheduled mission, the best-fitting RedEmP is selected from the database based on aircraft type, air distance, initial cruise flight level, and seat load factor. This profile is then projected onto the horizontal flight trajectory. To obtain a more realistic vertical distribution of aviation emissions using mission-specific ADS-B data, the vertical structure of the selected RedEmP is subsequently adapted to the observed flight profile. For this purpose, an initial RedEmP with a constant cruise altitude corresponding to the dominant cruise altitude of the ADS-B trajectory is selected based on mission-specific air distance and seat load factor. In a first step, the top-of-climb and top-of-descent points are identified by analysing climb and descent rates as well as the duration of constant-altitude segments. Subsequently, each waypoint along the flight trajectory is assigned to a corresponding RedEmP flight phase according to its altitude, thereby preserving the underlying flight-physics characteristics of the original RedEmP. For waypoints assigned to the cruise phase, the altitude difference between the actual ADS-B flight profile and the cruise flight level of the selected RedEmP is determined. The corresponding cruise emission flows are then scaled using cruise emission data from the RedEmP with the best-matching cruise flight level.

3. Results

Firstly, the global results for aviation are presented (section 3.1) and the impact of cargo traffic is derived (section 3.2). Thereafter, the impact of airspace closures on specific missions is discussed (section 3.3) before completing with a comparison of this inventory with scheduled commercial passenger air traffic and alternative emission inventories. (section 3.4). Subsequent analyses are restricted to flights for which emission computations were successfully executed.

3.1 Global results

The global emission inventory for CO_2 is displayed in Figure 1 and the global results, for all analysed properties, are displayed in Table 1. In total 40.2 million flights are covered in the ADS-B dataset which cover a distance of 57.4 billion kilometers. In total, 79 % of all flights were performed by turbofan, 7 % by turboprop and 14 % by piston aircraft using a total of 244.3 megatons of jet fuel. Although cargo aircraft perform only 2.8 % of all flights, they account for 9.9 % of total jet fuel consumption.

The altitude-longitude distribution of the annual emissions is displayed in Figure 2. There are three main clusters: North America, Europe and China, while minor clusters get visible in the Middle East and India. The intercontinental connections in cruise altitude get visible well while the Brazilian east

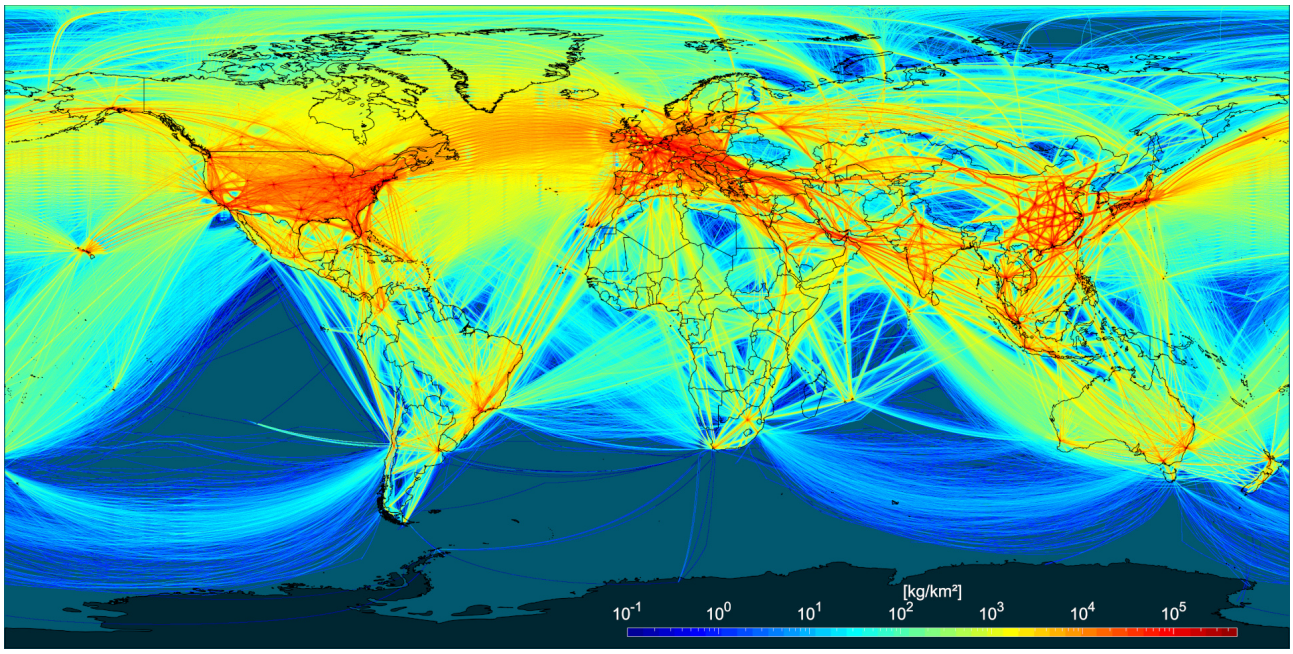


Figure 1 – Latitude-Longitude distribution of the vertically aggregated aviation CO_2 emissions for year 2023.

Table 1 – Annual statistics of global air traffic in 2023.

	Total	Of which			
		Turbofan	**Turboprop**	**Piston**	**Cargo**
Number of flights	40 165 650	31 744 713	2 681 027	5 739 877	1 125 919
Track distance [x10^9km]	57.41	54.93	1.16	1.31	3.10
Fuel consumption [Mt]	244.3	242.5	1.57	0.186	24.26
Fuel per km [kgkm^{-1}]	4.25	4.41	1.35	0.14	7.82
Mean distance [km]	1 429	1 730	433	229	2 755
Mean flight time [s]	6 935	7 992	3 338	2 766	12 014
CO_2 [Mt]	771	766	4.97	0.587	76.65
H_2O [Mt]	300	298	1.93	0.228	29.84
NO_x [Mt]	3.71	3.69	0.0169	0.000802	0.354
nvPM mass [kt]	7.48	7.36	0.093	0.027	0.394
nvPM number [x10^{25} #]	8.15	8.04	0.105	0.0049	0.524
Cargo share [%]	9.93	9.99	1.89	0	-

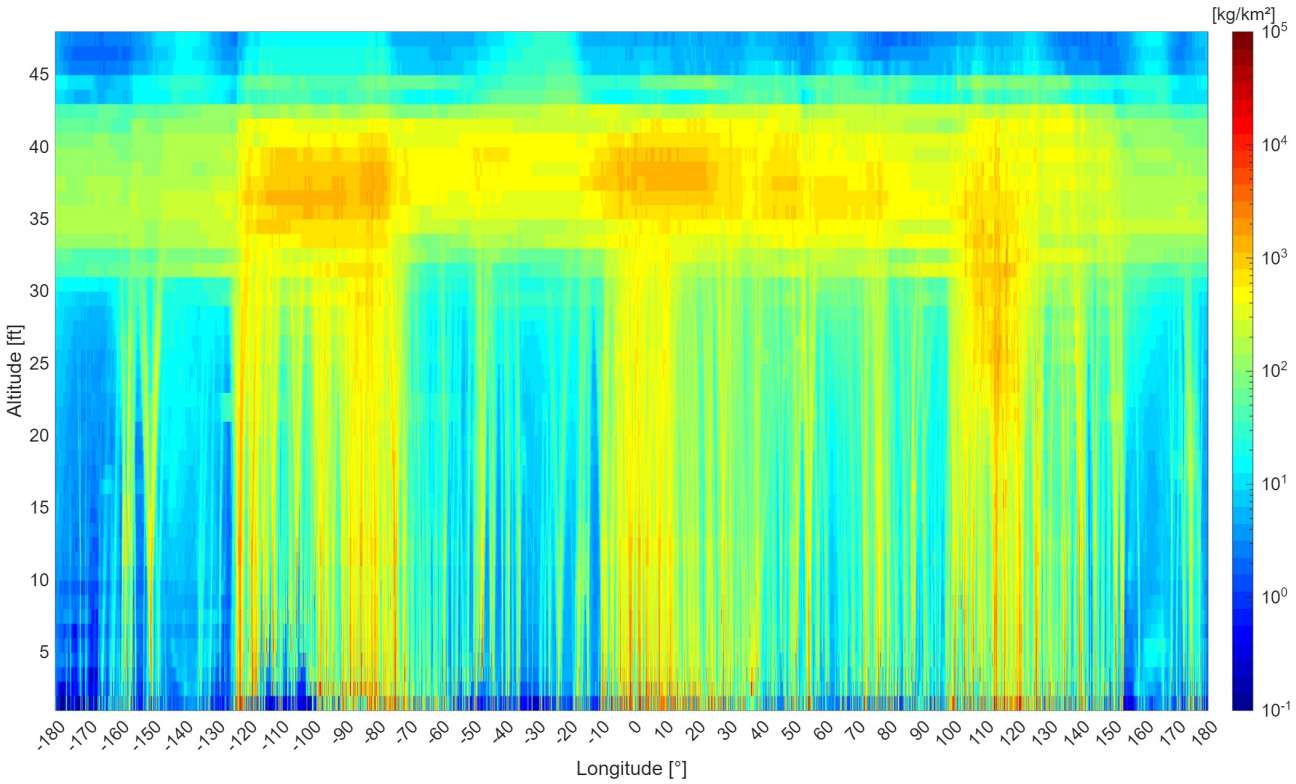


Figure 2 – Meridional annual CO_2 emissions from aviation for year 2023, zonally aggregated and in dependence of the emission pressure altitude and longitude.

coast marks the start of the American continent in ground proximity. The Hawaiian islands and Anchorage are extremely visible due to their remote location in an otherwise not greatly used area other than cruise. While Europe and North America have a similar altitude profile, which is more oriented to the fuel optimal cruise altitude, China's altitude profile is on average about 6.000 ft lower and higher altitudes (flight level (FL) 330 and above) are less dense. Between FL290 and FL410 reduced vertical separation minima (RVSM) apply which leads to the usage of each FL. Above FL410, the minimum separation is set to 2.000 ft which leads to an unavailability of FL420 and FL440. FL410 and above are mainly used by business aviation and modern wide-body aircraft such as the Boeing B787- and Airbus A350 series. The latter's having a maximum service ceiling of FL430 leads FL430 to be the last flight level with visible cruise segments.

3.2 Cargo air traffic

Unless otherwise stated, the following analyses considers only dedicated freighter operations and excludes belly cargo transported in passenger aircraft. As discussed in section 3.1, global cargo traffic accounts for nearly 10 % of annual aviation fuel consumption and, consequently, of CO_2 emissions. However, due to the lack of comprehensive global databases, detailed cargo flight plans can currently only be derived from ADS-B data. While aggregate estimates of fuel consumption from cargo aviation may be available, such data are insufficient for bottom-up traffic forecasting and climate impact assessments. This is because future cargo traffic growth is expected to be spatially and operationally heterogeneous [28], while accurate climate effect calculations additionally require information on the spatial and temporal distribution of emissions. A global annual emission inventory for cargo air traffic is displayed in Figure 3. Global fuel demand in 2023 is estimated to be 24.3 Mt, corresponding to CO_2 emissions of 76.7 Mt. Total NO_x emissions are approximately 0.354 Mt, equivalent to an average emission index of 14.8 $\frac{g_{NO_x}}{kg_{fuel}}$. Cargo flights account for about 3 % of all flights, while the mean stage length increases from 1 426 km for passenger aviation to 2 755 km for cargo transport. Major cargo routes are listed in Table 2. OD-pairs and dominant aircraft types differ substantially from passenger operations, with Anchorage International Airport (PANC) serving as a key transpacific cargo hub. In total, 10 162 unique connections were served.

Table 2 – Main cargo air traffic routes by number of flights.

Pos.	Origin	Destination	Number flights	Most frequent aircraft	Agg. flight dist. [Mio. km]
1	Hong Kong (VHHH)	Anchorage (PANC)	5 691	B748(F), B744(F)	50.1
2	Anchorage (PANC)	Chicago (KORD)	5 475	B744(F), B77L(F)	26.19
3	Bogotá (SKBO)	Miami (KMIA)	4 507	B763(F), A332(F)	11.51
4	Seoul (RKSI)	Anchorage (PANC)	3 782	B744(F), B77L(F)	26.14
5	Anchorage (PANC)	Seoul (RKSI)	3 190	B744(F), B77L(F)	21.61
6	Anchorage (PANC)	New York (KJFK)	3 157	B744(F), B77L(F)	18.05

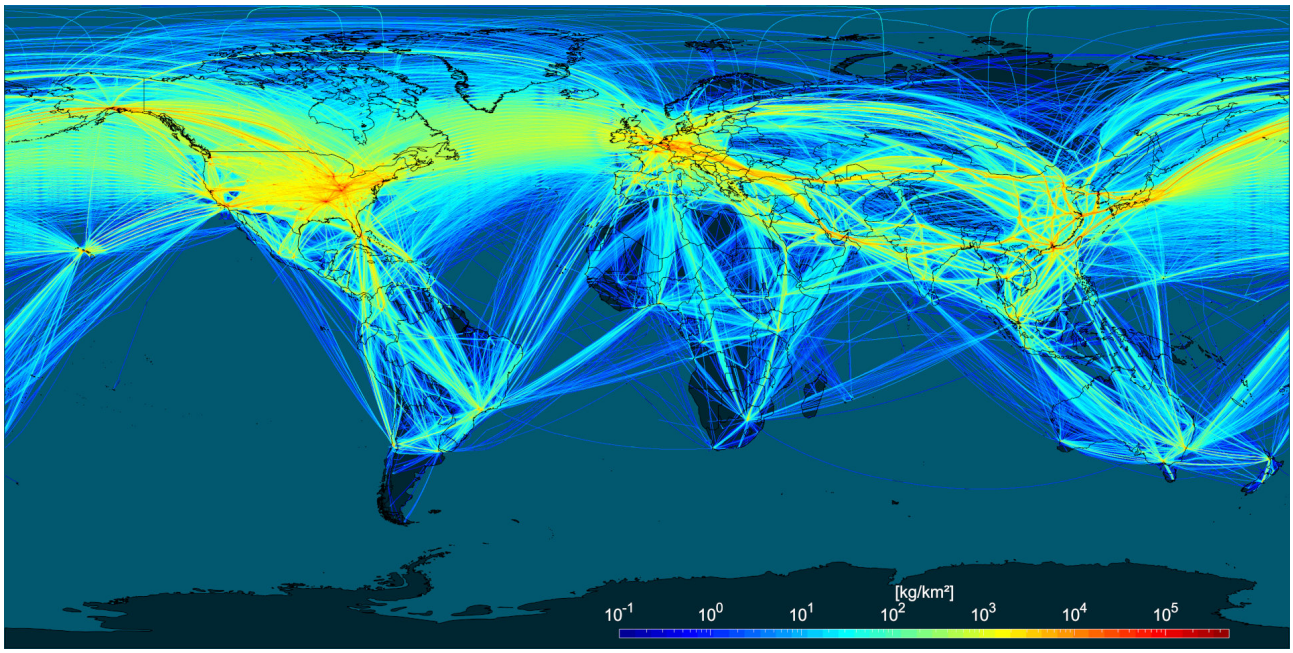
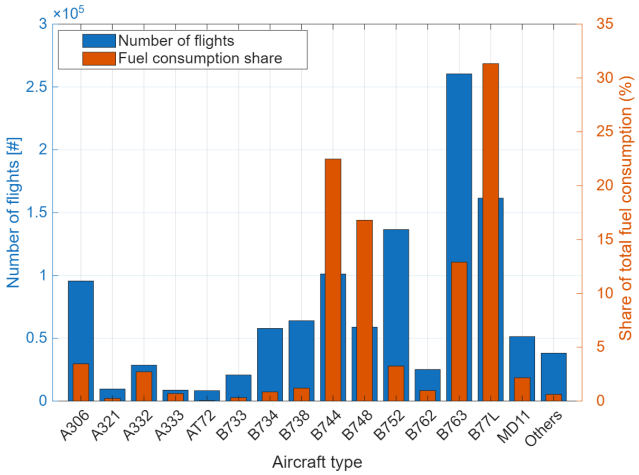


Figure 3 – CO_2 emission inventory for global cargo air traffic in 2023.

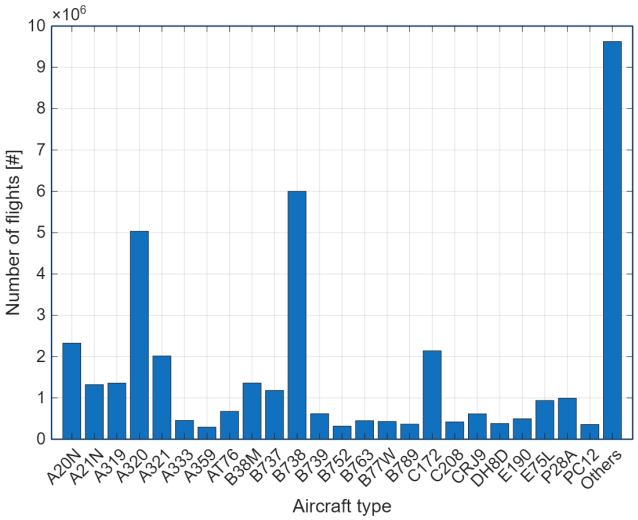
Overall, the cargo fleet comprises a higher share of wide-body aircraft than passenger aviation. Figure 4a displays the absolute number of flights performed by each cargo aircraft as well as the relative share of their fuel consumption of all cargo flights and Figure 4b the number of flights per aircraft type for the global flight plan. While narrow-body aircraft overall dominate the number of flights, the cargo segment is dominated by wide-body and larger narrow-body aircraft (e.g. B752). If considering the fuel consumption as relative metric, wide-body aircraft account for almost the complete cargo air traffic fuel consumption.

Figure 5 illustrates the fuel consumption associated with the most significant country pairs in global cargo aviation. Domestic cargo air traffic within the United States accounts for approximately 5.2 Mt of fuel consumption, corresponding to 21 % of total global cargo aviation fuel use. Routes originating from or destined for the United States dominate global cargo aviation fuel consumption, with the United States being involved in approximately 46 % of total cargo aviation fuel consumption when both departing and arriving flights are considered.

The most relevant cargo airports in terms of fuel consumption (inbound and outbound) are displayed in Table 3 while Table 4 shows the main cargo airports in terms of cargo volume according to [29] (the latter might include belly cargo). Eight of the ten most important cargo airports, ranked by fuel consumption and cargo volume, are identical while 5 are situated at the Pacific ocean. Cargo flights arriving at and departing from PANC account for approximately 9 % of global cargo aviation fuel consumption. Furthermore, the ten largest cargo airports are responsible for 39.5 % of total cargo aviation fuel consumption, underlining the importance of major intercontinental cargo hubs for global air freight operations. For all flight operations combined, the ten airports with the highest fuel consumption are responsible for only 17 % of global aviation fuel consumption, indicating a substantially



(a) Number of flights per cargo aircraft type and share of total cargo aviation fuel consumption.



(b) Number of detected flights per aircraft type in 2023.

Figure 4 – Aircraft statistics for global air traffic

Table 3 – Main cargo airports by fuel consumption (inbound and outbound)

Airport	Fuel [Mt]	Flights [#]	Distance [mn. km]
PANC	4.313	77 210	453.1
VHHH	3.018	64 205	316.2
RKSI	2.129	46 667	215.2
ZSPD	1.636	36 032	189.7
KMEM	1.616	123 742	275.9
KLAX	1.433	31 996	169.5
KSDF	1.3	92 679	179.3
KORD	1.149	27 259	125.7
KMIA	1.063	50 455	147.9
KCVG	1.033	48 287	140.9

Table 4 – Main cargo airports by cargo volume [29]

Airport	Cargo volume [t]
VHHH	4 331 976
KMEM	3 881 211
ZSPD	3 440 084
PANC	3 380 374
RKSI	2 744 136
KSDF	2 727 820
KMIA	2 525 591
OTHH	2 355 503
KLAX	2 130 835
RCTP	2 112 988

less concentrated distribution than for dedicated cargo operations.

3.3 Geopolitical events

While transatlantic and transpacific air traffic can generally utilize a broad range of routing options, air traffic between Europe and Asia is constrained to a limited number of major airways located in close proximity to restricted airspaces resulting from geopolitical sanctions and active conflict zones. Consequently, flights on these routes are often forced to follow substantial detours, leading to increased ground and air distances relative to the corresponding great-circle distance. The deviation between actual air- and great-circle distance for 10 major European, 10 major East Asian, and 10 major North American airports is illustrated in Figure 6. Figure 6a presents the direction-dependent deviation between air- and great-circle distance for city-pairs with more than 100 annual flights. A pronounced directional asymmetry can be observed, primarily driven by prevailing jet streams that flow from west to east. Eastbound flights frequently exhibit shorter air distances relative to the great-circle distance due to strong tailwinds, whereas westbound flights are subject to increased air distances caused by persistent headwinds. In contrast to the relatively unrestricted routing of traffic between Europe and North America, flights between Europe and East Asia are heavily affected by airline-specific airspace limitations. In particular, routes serving Japan (RJTT and RJAA) and South Korea (RKSI) experience significant operational impacts, as most airlines operating these services are prohibited from utilizing Russian airspace. If not considering the direction (see Figure 6b), direction dependent effects for

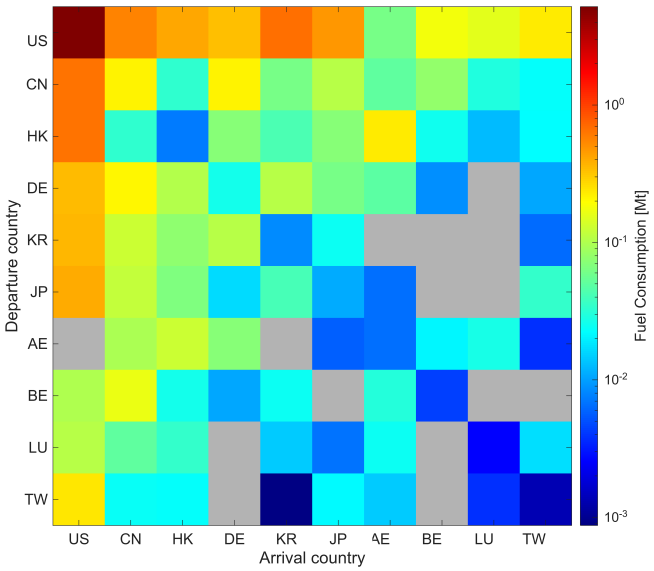
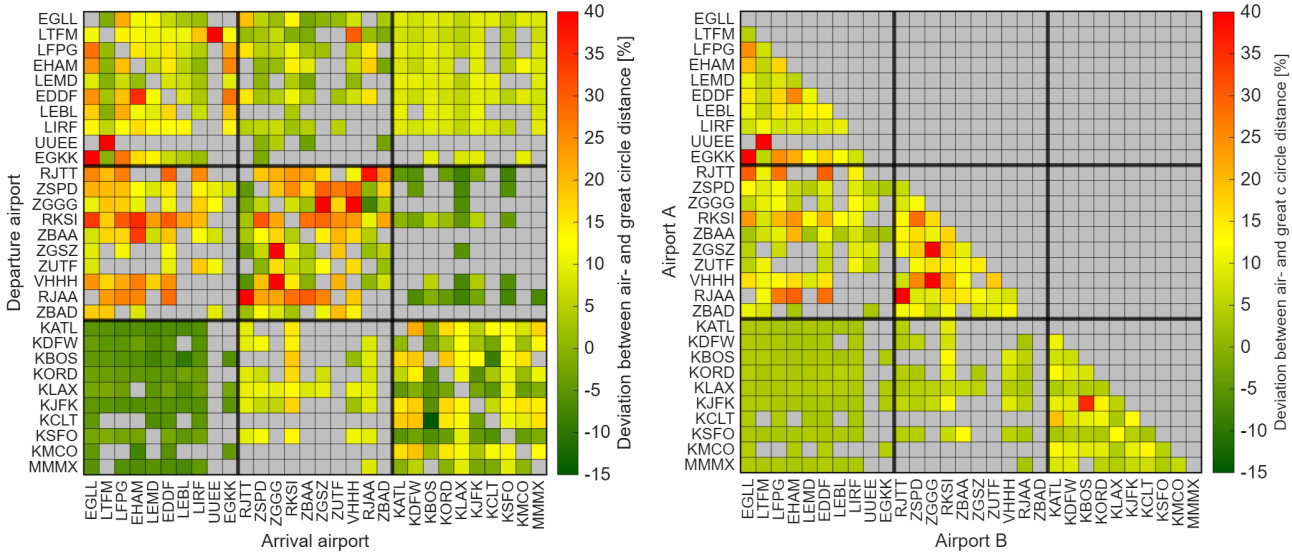


Figure 5 – Fuel consumption for the most relevant country pairs in cargo air traffic. Countries are abbreviated with their two-letter ISO code.

North-Atlantic routes offset each other well, while continental routes do not.
Geopolitical conflicts get visible in emission inventories quite well. Figure 1 shows the global emission inventory. There is almost no traffic over Libya and Ukraine (The visible emissions over closed airspace are an artifact of ADS-B data gaps, where missing trajectory segments are approximated by great-circle routes). In 2023 the Afghan airspace was still avoided and the north-east corridor gets visible well. Although the FAA lifted a ban to overfly Afghan airspace in mid-2023, airlines first started re-using Afghan airspace in mid-2024. On an airline basis it is furthermore possible to analyse airline specific restrictions due to geopolitical tensions (e.g. Western airlines are prohibited to overfly Russian airspace and Royal Air Maroc is prohibited to overfly Algerian airspace). The resulting data can be used to analyze the competitiveness of different airlines.

3.4 Discussion and comparison

The here presented inventory is the first bottom-up 4D-inventory published for 2023. The International Energy Agency (IEA) estimates aviation's CO_2 emission to be 940.6 Mt in 2023 [30] which corresponds to a kerosene consumption of 297.7 Mt and is 18 % higher than the here presented consumption. Similar bottom-up studies from other years, based on ADS-B data, range from -7 % [4] to -12 % [3] compared to IEA data. Quadros et al. uses Flightradar24 and Teoh et al. and the here presented inventory Spire Global as data source. The explanation why the fuel consumption is below the IEA data has multiple reasons. Firstly, approximately 5 % of all commercial flight kilometers were excluded from the analysis, as the corresponding flights failed to fulfill the predefined quality criteria. The two major problems were (i) the extrapolated distance between the first/ last waypoint and the, from the flight plan obtained, origin and destination airport was too long; (ii) Either departure or arrival airport are not detected and the schedule contains no information about the scheduled departure and destination airports. For general aviation aircraft, the discrepancy is substantially greater, with the underestimation reaching approximately 50 %. However, the total underestimation of general aviation cannot be adequately quantified because (i) many general aviation aircraft are not required to be equipped with ADS-B transponders; (ii) the coverage of general aviation traffic within the underlying ADS-B dataset is unknown and can not be quantified sufficiently. Additionally, the underestimation of small general aviation aircraft might increase significantly when using other data sources. Secondly, military and governmental flight operations are only partially captured, as inclusion requires both the availability of ADS-B trajectory data and an appropriate flight performance model. Consequently, only a subset of such operations can be represented, while coverage is largely restricted to the military's civil aircraft that might transmit ADS-B data and are not blocked. Thirdly, engine degradation effects were not considered.



(a) Mean deviation between air- and great circle distance direction-dependent.

(b) Mean deviation between air- and great circle distance direction-independent.

Figure 6 – The mean deviation between air- and great circle distance between different OD-pairs in Europe, Asia and North-America. Grey box color indicates that no data or no representative data is present.

In comparison, a bottom-up inventory (for comparison purposes) based on Sabre Market Intelligence flight plan data, combined with range-, aircraft-, and load-factor-dependent regression models derived from BADA 4.2 [31] and statistical detour factors for range estimation, reports a total fuel consumption of 230 Mt and a total flown distance of 52.83 bn km. These values are 5.7 % and 9.2 % lower, respectively, than those obtained in the present inventory. Given that the inventory presented here additionally includes cargo and general aviation traffic, the difference in fuel consumption would be expected to be closer to 10 % or higher. This suggests that the fuel consumption reported for commercial passenger aviation in the present inventory is underestimated. A likely explanation is the exclusion of flights that did not meet the required data quality criteria and were therefore omitted from the analysis.

The most current bottom-up emission estimation was performed by Dannet et al. [32] which uses flight plan data obtained by Flightradar24 in combination with the fuel estimation in air transport (FEAT) model [33] (Regression formulas based on BADA) and average- range dependent deviations between ground- and great circle distance. Wind is not considered. It estimates the global fuel consumption in 2023 to be 261 Mt with a total distance flown of 57.1 bn km which is a 7 % higher fuel consumption and 1 % shorter distance flown than the here presented data. The difference can be explained with a slightly different aircraft type distribution, the method used for fuel estimation and flight distance and the consideration of wind effects. Furthermore, Dannet et al. have a 7 % larger number of flights considered in their inventory. It can be assumed that the emission amounts are highly dependent on the used data sources for the flight plan as well as trajectory data. Uncertainties of the methods used to compute the here presented inventory, especially linearisation of the RedEmP's, the underlying flight performance model BADA, fuel flow correlation methods and the sensitivity of the load factor, are discussed in detail in Righi et al. [6].

4. Conclusion and Outlook

In this paper, a global aviation emission inventory for the year 2023 was developed based on ADS-B data provided by Spire Global. The inventory incorporates ERA5 reanalysis meteorological data and fuel-flow-based methods to estimate additional emission species, including CO_2 NO_x, SO_2, HC, OC, soot, nvPM mass, and nvPM number. The resulting dataset comprises 40.2 million identifiable flights for which suitable flight performance models are available. Of these flights, 79 % were operated by turbofan aircraft, 6.7 % by turboprop aircraft, and 14.3 % by piston-engine aircraft. In total, global

aviation consumed 244.3 Mt of kerosene, resulting in emissions of 771 Mt of CO_2, 300 Mt of H_2O, 3.71 Mt of NO_x, and 7.48 kt of nvPM. Global cargo aviation accounted for only 2.85 % of all flights, but contributed approximately 10 % of total aviation fuel consumption. While transoceanic missions generally exhibit comparatively low lateral inefficiencies, continental flights between Europe and Asia can be subject to substantial detours due to ongoing conflicts and associated restrictions in airspace availability. Given the current geopolitical situation and the limited number of available airways between Europe and Asia, it would be valuable to simulate a hypothetical closure of the remaining air corridors over Armenia, Azerbaijan, and the Middle East, and to assess the resulting impacts on global aviation. Future improvements include the integration of uncertainty quantification for NO_x and nvPM emissions as well as better calculation and rastering of taxi emissions.

5. Acknowledgements

The authors thank colleagues from the DLR Institute of Air Transport for providing information about scheduled passenger traffic and global fleet information, colleagues from the DLR Institute of Flight Guidance for providing the ADS-B dataset and colleagues from the DLR Institute of System Architectures in Aeronautics for providing aircraft design data. We kindly thank all external data suppliers for providing the input data for aviation emission modelling (specifically Spire Global, ECMWF, EUROCONTROL, Sabre and Cirium). The here presented emission inventory has been created with elements of BADA Family 4 Release 4.2 which has been made available by EUROCONTROL to DLR e.V. EUROCONTROL has all relevant rights to BADA © 2021. The European Organisation for the Safety of Air Navigation (EUROCONTROL). All rights reserved. EUROCONTROL shall not be liable for any direct, indirect, incidental or consequential damages arising out of or in connection with this product or document, including with respect to the use of BADA. The here used, pre-computed, BADA 4.2 RedEmP's were created for the DLR project "Emissionslandkarte" (ELK).

6. Data availability

The annual and daily emission inventories containing CO_2, H_2O, NO_x, OC, nvPM mass, nvPM number, Soot, SO_2, HC, CO and travelled distance per grid cell can be made available upon request for total or cargo air traffic. The resolution is $0.125^\circ \times 0.125^\circ \times 1\,000$ ft. Single flight emission inventories and results, as well as precise schedule data, can not be made available. Flight performance and raw ADS-B data as well as used software can not be made available.

7. Contact Author Email Address

maximilian.clococeanu@dlr.de

8. Copyright Statement

The authors confirm that they, and/or their company or organization, hold copyright on all of the original material included in this paper. The authors also confirm that they have obtained permission, from the copyright holder of any third party material included in this paper, to publish it as part of their paper. The authors confirm that they give permission, or have obtained permission from the copyright holder of this paper, for the publication and distribution of this paper as part of the ICAS proceedings or as individual off-prints from the proceedings.

References

[1] D.S. Lee, D.W. Fahey, A. Skowron, M.R. Allen, U. Burkhardt, Q. Chen, S.J. Doherty, S. Freeman, P.M. Forster, J. Fuglestvedt, A. Gettelman, R.R. De León, L.L. Lim, M.T. Lund, R.J. Millar, B. Owen, J.E. Penner, G. Pitari, M.J. Prather, R. Sausen, and L.J. Wilcox. The contribution of global aviation to anthropogenic climate forcing for 2000 to 2018. *Atmospheric Environment*, 244:117834, 2021.

[2] A. Leipold, F. Baier, U. Bauder, J. Blinstrub, K.A. Buchtal, E. Campillo Borras, M. Clococeanu, G. Eckel, D. Ennen, N. Flüthmann, M. Gelhausen, T. Hoff, M. Kühlen, S. Kumar, A. Link, P. Ratei, S. Ruoff, R. Schmid, and L. Weber. Depa 2070 – development pathways for aviation up to 2070 (final report). Technical report, 2025.

[3] R. Teoh, Z. Engberg, M. Shapiro, L. Dray, and M. E. J. Stettler. The high-resolution global aviation emissions inventory based on ads-b (gaia) for 2019–2021. *Atmospheric Chemistry and Physics*, 24(1):725–744, 2024.

[4] F.D.A. Quadros, M. Snellen, J. Sun, and Irene C Dedoussi. Global civil aviation emissions estimates for 2017–2020 using ADS-B data. *J. Aircr.*, 59(6):1394–1405, November 2022.

[5] J. Klenner, H. Muri, and A.H. Strømman. Domestic and international aviation emission inventories for the unfccc parties. *Environmental Research Letters*, 19(5):054019, apr 2024.

[6] M. Righi, S. Ehrenberger, S. Brinkop, J. Hendricks, J. Hellekes, P. Banyś, I. Dasgupta, P. Draheim, A. Fitz, M. Löber, T. Pregger, Y. Scholz, A. Schulz, B. Suhr, N. Thomsen, C. M. Weder, P. Berster, M. Clococeanu, M. Gelhausen, A. Lau, F. Linke, S. Matthes, and Z. L. Zengerling. The elk global emission inventory for the transport sectors. *Earth System Science Data*, 18(2):1619–1664, 2026.

[7] A. Leipold, G. Aptsiauri, A. Ayazkhani, U. Bauder, R.G. Becker, R. Berghof, A. Claßen, A. Dadashi, K. Dahlmann, N. Dzikus, N. Flüthmann, V. Grewe, L. Göhlich, W. Grimme, Y. Günther, R. Jaksche, M. Jung, F. Knabe, P. Kutne, P. Le Clercq, H. Pabst, S. Poggel, M. Staggat, K. Wicke, F. Wolters, J. Zanger, and T. Zill. Depa 2050 – development pathways for aviation up to 2050 (final report). Technical report, 2021.

[8] Z.L. Zengerling, S. Kumpa, M. Clococeanu, M. Mendiguchía Meuser, J. Solzer, and K. Dahlmann. Assessing climate effects resulting from airspace closures following the ukrainian crisis. *Journal of Open Aviation Science*, 2(2), Sep. 2025.

[9] Spire Global Inc. Ads-b, 2024. `https://spire.com/spirepedia/ads-b/`. Accessed: 07 January 2026.

[10] Sabre GLBL Inc. Sabre market intelligence, 2026. `https://www.sabre.com/products/suites/pricing-and-revenue-optimization/market-intelligence/`. Last accessed: 07 January 2026.

[11] Cirium. Cirium fleets analyzer. Technical report, Cirium, London, UK, 2023. last access: 12 May 2026.

[12] Copernicus Climate Change Service. ERA5 hourly data on pressure levels from 1940 to present, 2023. `https://cds.climate.copernicus.eu/datasets/reanalysis-era5-pressure-levels?tab=overview`. Accessed: 07 January 2026.

[13] F. Linke. Ökologische analyse operationeller lufttransportkonzepte. Technical report, Technische Universität Hamburg-Harburg, 2016.

[14] Z. L. Zengerling, F. Linke, C.M. Weder, S. Dietmüller, S. Matthes, and P. Peter. Flying low and slow: Application of algorithmic climate change functions to assess the climate mitigation potential of reduced cruise altitudes and speeds on different days. *Meteorologische Zeitschrift*, pages 1–15, September 2023.

[15] A. Nuic, D. Poles, and V. Mouillet. Bada: An advanced aircraft performance model for present and future atm systems. *International Journal of Adaptive Control and Signal Processing*, 24(10):850–866, 2010.

[16] S. Woehler, G. Atanasov, D. Silberhorn, B. Fröhler, and T. Zill. Preliminary aircraft design within a multidisciplinary and multifidelity design environment. 04 2020.

[17] D.I.A. Poll and U. Schumann. An estimation method for the fuel burn and other performance characteristics of civil transport aircraft during cruise: part 2, determining the aircraft's characteristic parameters. *The Aeronautical Journal*, 125(1284):296–340, 2021.

[18] F. Linke, V. Grewe, and V. Gollnick. The implications of intermediate stop operations on aviation emissions and climate. *Meteorologische Zeitschrift*, 26(6):697–709, 12 2017.

[19] Z.L. Zengerling, F. Linke, C.M. Weder, and K. Dahlmann. Climate-optimised intermediate stop operations: Mitigation potential and differences from fuel-optimised configuration. *Applied Sciences*, 12(23), 2022.

[20] M.d.J. Gurrola Arrieta, R.M. Botez, and A. Lasne. An engine deterioration model for predicting fuel consumption impact in a regional aircraft. *Aerospace*, 11(6), 2024.

[21] J. T. Wilkerson, M. Z. Jacobson, A. Malwitz, S. Balasubramanian, R. Wayson, G. Fleming, A. D. Naiman, and S. K. Lele. Analysis of emission data from global commercial aviation: 2004 and 2006. *Atmos. Chem. Phys.*, 10(13):6391–6408, jul 2010.

[22] CRC. Update of the survey of sulfur levels in commercial jet fuel: Final report. Technical Report 605, CRC Project AV-1-10, Coordinating Research Council, 2012.

[23] D. DuBois and G.C. Paynter. "fuel flow method2" for estimating aircraft emissions. In *SAE Technical Paper 2006-01-1987*. SAE International, August 2006.

[24] EASA. Icao aircraft engine emissions databank version 31, 2025. `https://www.easa.europa.eu/en/domains/environment/icao-aircraft-engine-emissions-databank`. Last accessed: 07 January 2026.

[25] F. Deidewig, A. Doepelheuer, and M. Lecht. Methods to assess aircraft engine emissions in flight. In *20th Congress of the Int. Council of the Aeronautical Sciences 1996 (ICAS), 8-13 Sept. 1996, Sorrent, Italien*, pages 131–141, 1996. LIDO-Berichtsjahr=1996, note=Schadstoffe in der Luftfahrt, pages=11,.

[26] D. Ahrens, B. Kim, Y. Méry, J. Zelina, R. Dudebout, and R. Miake-Lye. The aircraft nvpm mission emis-

sions estimation methodology, version 2 (meem2). 10 2025.

[27] A. Agarwal, R.L. Speth, T.M. Fritz, S.D. Jacob, T. Rindlisbacher, R. Iovinelli, B. Owen, R.C. Miake-Lye, J.S. Sabnis, and S.R. H. Barrett. Scope11 method for estimating aircraft black carbon mass and particle number emissions. *Environmental Science & Technology*, 53(3):1364–1373, 2019.

[28] F. Baier, P. Berster, and M. Gelhausen. Global cargo gravitation model: airports matter for forecasts. *Int. Econ. Econ. Pol.*, 19(1):219–238, 2022.

[29] Top 10 busiest airports in the world shift with the rise of international air travel demand | ACI World — aci.aero. `https://aci.aero/2024/04/14/top-10-busiest-airports-in-the-world-shift-with-the-rise-of-international-air-travel-demand/`. Last accessed: 07-06-2026.

[30] International Energy Agency. Aviation. `https://www.iea.org/energy-system/transport/aviation`. Accessed: 2026-05-16.

[31] I. Mayeres, E. Peduzzi, M. Alder, F. Baier, K.A. Buchtal, S. Chatterjee, M. Clococeanu, D. Ennen, M. Gelhausen, A. Junior, A. Leipold, P. Shiva Prakasha, P. Ratei, and T. Zengerling, Z.L.and Lefebvre. Assessing policies for the uptake of sustainable aviation fuels using the impact monitor framework. *Engineering Proceedings*, 90(1)(95), April 2025.

[32] G. Dannet, O. Boucher, and N. Bellouin. Features and evolution of civil aviation co_2 emissions based on ads-b data for the period between 2019–2024. *Metascience in Aerospace*, 1(4):346–370, 2024.

[33] K. Seymour, M. Held, G. Georges, and K. Boulouchos. Fuel estimation in air transportation: Modeling global fuel consumption for commercial aviation. *Transportation Research Part D: Transport and Environment*, 88:102528, 2020.